Investigations of the turbulent thermo-fluid performance in a circular heat exchanger with a novel flow deflector-type baffle plate

Md Atiqur RAHMAN [ID]* and Sushil Kumar DHIMAN

Department of Mechanical Engineering, Birla Institute of Technology, Mesra, Ranchi, India

Abstract. An axial flow tubular heat exchanger has been experimentally investigated to augment the heat transfer rate with a novel swirl flow of air past the heated tubes. The novel design has been based on circular baffle plates provided with trapezoidal air deflectors of various inclination angles. The arrangement of tubes is kept the same throughout the experiment, in accordance with the longitudinal airflow direction. The tubes maintained a constant heat flux condition over the surface. Four deflectors with equal inclination angles were developed on each baffle plate, generating air swirl inside a circular duct carrying the heated tubes that increase air-side turbulence and, consequently, the surface heat transfer rate. The baffle plates were placed equidistant from each other at variable pitch ratios. The Reynolds number was kept in the range of 16000–28000. The effect of pitch ratios and inclination angles on the thermo-fluid performance of the heat exchanger was studied. The investigations revealed an average improvement of 3.75 times in thermo-fluid performance for an exchanger with a deflector baffle plate with a baffle inclination angle of 50° and a pitch ratio of 1.4 when compared to other inclination angles and pitch ratios.

Key words: thermo-fluid performance; flow resistance; swirl flow; re-circulation; trapezoidal deflector; inclination angle.

1. INTRODUCTION

A global increase in energy demand and climate change have led researchers to emphasize energy conservation, utilization and recovery techniques. In the last several years, numerous strategies for enhancing heat transfer theories have been implemented in various heat exchanger (HX) applications, for instance, in the processing industry, refrigeration, solar water heaters, etc. [1]. Strategies for enhancing heat transfer are usually divided into three categories [2, 3], i.e. active, passive and compound methods, with the common objective of reducing thermal boundary layer thickness to attain an effective surface heat transfer coefficient. Passive methods generally include extended surfaces, surface roughness, liquid and gas additives, surface coating, swirl flow devices, twisted (convoluted) tubes, etc. The active method necessitates additional external power sources. Mechanical aids, surface-fluid vibration, swirl flow-turbulator devices, fluid injection and suction, electrostatic fields and jet impingement are a few examples. Passive methods are extensively studied, due to easy maintenance, low cost, and non-reliability on an external power source, thus gaining popularity. These enhancement techniques mainly reduce thermal resistance by generating turbulence inside the flow field or increasing the heat transfer surface area [4].

The turbulator or reverse flow device is frequently used for heat transfer enhancement applications. Reverse flow is also known as "recirculation flow". Boundary layer dissipation and flow reversal enhance the momentum transfer rate and heat transfer coefficient. Increasing the axial Reynolds number (Re) adequately, reducing the flow cross-section area, raising average velocity or temperature gradient and flow reversal. along with high turbulence, can all accelerate tube wall convection. The significant effective driving potential force and higher-pressure drop can enhance heat fluxes and a higher momentum transfer. Many heat transfer applications, like gas turbine blades, HXs, combustion chambers and cooling of electronic devices, are concerned with the intensity of reverse flow and the reconnecting position.

Yakut and Sahin [5] created reverse/turbulent flows within each conical ring's module using conical-ring turbulators placed inside the tube. As a result, heat transfer along the tube wall was improved. Different intensities of reverse flow (recirculation flow) were generated in their experimental study by separating/reattachment of the boundary layer between modules with varying pitch lengths. Similar work involving a circular ring turbulator [6] with a Re_d (Reynolds number) range of 4000–23000, a diameter ratio (DR) varying along the scale of 0.5–0.8, and a pitch ratio (P_R) of 1–4 showed the highest heat transfer rate at lower P_R and D_R.

Furthermore, the swirl flow generator improves heat transfer in various engineering applications. Swirl flow is widely utilized in various industries to enhance heat and mass transfer in devices such as HXs [7], vortex combustors, drying processes, etc. Swirl flow devices come in two varieties: those with continuous swirl flow and with decaying swirl flow. Continuous swirling motion along the entire tube length is called continuous swirl flow, as in twisted-tape inserts [8, 9], coiled wires [10, 11] and helical grooves [12]. In the case of decaying

*e-mail: rahman.md4u@gmail.com

swirl flow, typically, the swirl motion is created at the tube's entry and degrades throughout the flow course [13–15]. Examples of its use include the tangential flow injection device and the radial guide vane swirl generator. The heat transfer coefficient and pressure drop of decaying swirl flow decrease with axial distance, whereas the heat transfer coefficient and pressure drop of continuous swirl flow remain constant. Discontinuous helical turbulator was reported in [16,17], with an open area ratio (0 and 0.0625), P_R (1.83, 2.92 and 5.83), and the Re_d range of 6000–12000. Higher thermal performance was observed at a higher open area ratio and lower pitch ratio.

Many researchers have investigated the swirl flow device. The methods for producing swirls are classified into three types [18]. The first method is tangential flow injection, where a tangential flow is introduced to induce a swirl fluid motion downstream [6, 13, 14, 19]. The second type of swirl generator is guide vanes [15, 20, 21], divided into two categories: radial and axial guide vanes. The last method involves direct rotation of the tube.

The above quoted literature showed heat transfer augmentation using different designs of turbulators. The focus was on swirl-generating devices to modify path lines and generate recirculation and streamlines, intensifying fluid mixing and generating higher turbulence within the flow regime.

Further research is therefore required to explore the different designs of turbulators focusing on HX application that can maximize heat transfer with minor changes in pressure drop. Furthermore, the thermo-fluid behavior of HXs with the baffle plate (equipped with the turbulator) is rare. Also, studies related to

working fluids such as air are limited in the above literature. In the current study, swirl generators (trapezoidal tangential flow deflector) are fitted on each baffle plate with a center distance of 40mm, generally located at the beginning of the test section. As a result, the swirl is quite intense at the entry and fades gradually along the flow downstream. This method increases velocity of the tangential flow. Also, it extends residence time in the tube, reducing the boundary layer thickness, while turbulent fluctuation in the tangential and radial directions increases, thereby increasing heat transfer in the duct fluid [14]. The study is carried out in a circular duct, with air-side heat transfer, and friction characteristics under forced convection. This experimental effort's primary objectives are to examine the variation in heat transfer and flow resistance caused due to (a) pitch ratio (P_R) variation of trapezoidal deflector baffle plates (DBP) and (b) inclination angle (α) variation. Four-pitch ratios $P_R = 0.8$, 1, 1.2 and 1.4 (pitch length to shell diameter ratio) are studied in the experiments. Along with the pitch ratio, three inclination angles, defined as the angle made by the deflector with the baffle plane, are used, i.e. $\alpha = 30°$, $40°$, and $50°$. All the experiments are conducted under similar inlet conditions with the Re_d (based on the D_h) range of 16 000–28 000. The results are compared to a smooth channel without DBP under a similar Re_d.

2. EXPERIMENTAL SETUP

Figures 1a and b depict the experimental setup, whose main components are HX, air supply, water-transfer loop, pressure and temperature instrumentations, and the data acquisition sys-
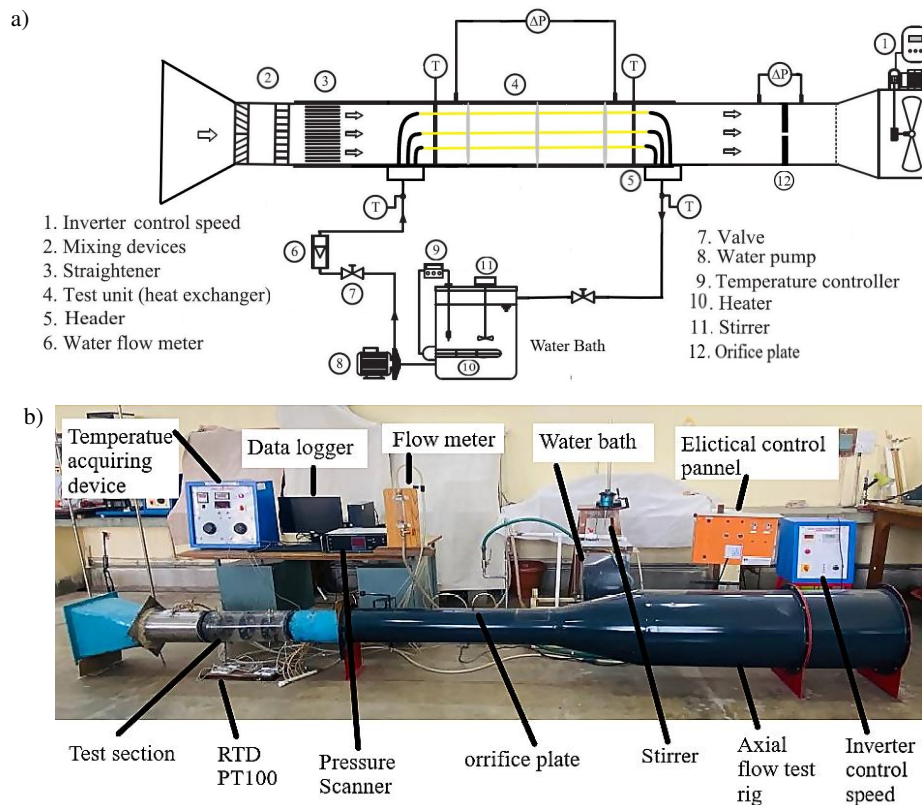

a)

1. Inverter control speed
2. Mixing devices
3. Straightener
4. Test unit (heat exchanger)
5. Header
6. Water flow meter
7. Valve
8. Water pump
9. Temperature controller
10. Heater
11. Stirrer
12. Orifice plate

Water Bath

b)

Temperatue acquiring device | Data logger | Flow meter | Water bath | Elictical control pannel

Test section | RTD PT100 | Pressure Scanner | orrifice plate | Stirrer | Axial flow test rig | Inverter control speed

Fig. 1. a) Schematic diagram of the experimental setup; b) Pictorial view of experimental setup

2

Bull. Pol. Acad. Sci. Tech. Sci., vol. 71, no. 4, p. e145939, 2023

www.czasopisma.pan.pl   PAN   www.journals.pan.pl
POLSKA AKADEMIA NAUK

Investigations of the turbulent thermo-fluid performance in a circular heat exchanger with a novel flow deflector-type baffle plate

tem. An open-type axial flow test rig was used to suck air through the HX. The atmospheric air was drawn employing a variable speed 2.2 kW inverter-controlled axial flow fan into the duct, which was then routed through the mixing device and straightener, and finally supplied to the HX. Thermocouple probes were located at the HX's air inlet ($T_{a,\text{in}}$) and outlet sections ($T_{a,\text{out}}$). The temperature was measured using 5 mm diameter probes inserted into the duct through which the air flowed. The probes used were T-type copper-constantan thermocouples grounded to a stainless-steel outer sheath. The temperature measuring positions selected were as recommended by the ASHRAE standard [22]. Change in temperature was constantly monitored and recorded. The temperature-measuring devices were calibrated using a standard precision mercury-in-glass thermometer in a controlled temperature bath. The airflow rate was estimated by using an orifice plate as suggested by the ISO 5801 standard. To measure the average air side pressure drop across the test section (ΔP), six pressure ports are generated by drilling 3 mm holes in the plexiglass (3 on the inlet and 3 on the exit side). The pressure port makes an angle of 120° with the center of the baffle plate. Both the pressure drop (ΔP) and the orifice plate (ΔP_0) were measured with a VDAS DAQ card, differential transducers of 0–1 psi, and a Lab view program. Airflow velocity is calculated using equation (2) on the basis of data from the orifice plate.

Heated water is held constantly at a temperature of 55°C with the help of 8 kW electrical heating elements and a thermostat (operating range: 40–300°C). Uniformity of fluid properties (like density and temperature) within the water bath is assured by utilizing mechanical stirrers. The hot water flow is regulated by employing a 0.25 hp feed pump, a bypass valve, and a rotameter. The hot water is then made available at a constant mass flow rate of 2LPM using a rotameter to a header from where it is uniformly distributed to the HX tube bundle. The tubes have been supported in the HX on baffle plates provided at a distinct pitch. The description of the baffle plates and the tube arrangement have been mentioned in the succeeding paragraph. PT100 RTDs have been utilized for measuring tube surface temperature, which carries hot water at different locations within the test setup.

During experimental testing, the water flow rate was fixed at a specific inlet water temperature while the airflow rate varied. The system was allowed to attain a steady state prior to recording data. After the system was stabilized, the temperatures at both inlet and outlet of the air passing through the heat exchanger and the surface temperature of copper tubes were measured. All tested conditions of the heat exchangers are shown in Table 1.

Table 1
Experimental operating conditions

| Air-inlet temperature, °C	32.5 ± 0.5
Air-inlet velocity, m/s	7–13
Water-inlet temperature, °C	55–60
Water mass flow rate, kg/s	0.03

The root mean sum square approach was used to estimate the accuracy of the direct measurement instrument shown in Table 2. The uncertainties, suggested by the Coleman and Steele's method [23], are shown in Table A1 in Appendix I.

Table 2
Accuracy of measurements

Parameters	Accuracy
Air temperature-inlet, °C	± 0.5
Pressure drops, Pa	± 0.1
Water temperature-inlet, °C	± 0.5
Water flow rate, kg/s	± 0.003

2.1. Test section details

The test section (circular duct), shown in Fig. 2, is made of Plexiglas, with thermal conductivity of $k_p = 0.2$ (W/mK), and its length is 60 cm with an ID of 19 cm and thickness of 0.5 cm. Copper tubes of thermal conductivity $k_t = 300$ (W/mK) with ID of 8 mm and thickness of 1 mm have been located in a channel parallel to it. They are given supports on baffle plates by sealing the tolerances at the supports. The copper tubes carry hot fluid, which may be liquid or gas. In contrast, the duct side fluid is the air taken from the ambient environment because this investigation is primarily based on air. Two sets of thermocouples measure the copper tube's surface temperature while carrying hot fluid, namely $T_{w,\text{in}}$, and $T_{w,\text{out}}$. Each set consists of five thermocouples, i.e. one attached to each tube, namely T_{w1}, T_{w2}, T_{w3}, T_{w4} and T_{w5}. A total of 5 thermocouples are used to capture the surface temperature of copper tubes at the inlet and outlet, as shown in Fig. 2. Additional thermocouples, $T_{a,\text{in}}$ at the inlet and $T_{a,\text{out}}$ at the exit, are provided to measure the air temperature as it enters and exits the test section.
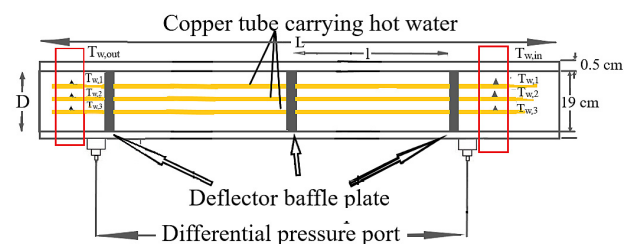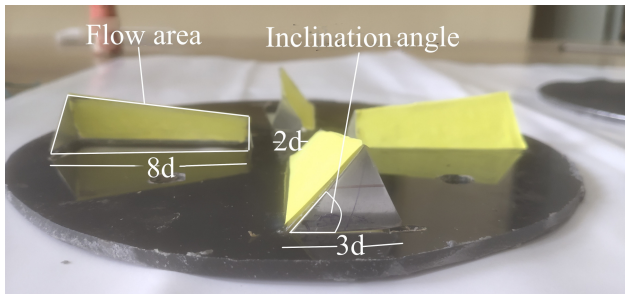

Fig. 2. Test section

2.2. Baffle plate and the arrangement of tubes

Figure 3 shows the novel deflector baffle plate (DBP) with five tube arrangements, one at the center and others arranged in a circular array at a distance of 4 cm from the center of the baffle plate.

The novel baffle plate has four trapezoidal openings that allow for air inflow to the duct. Four deflectors of the same dimension as the trapezoidal openings have been fixed at the desired angle to the baffle plate; this configuration helps to alter the airflow structures from axial to swirl flow.

Bull. Pol. Acad. Sci. Tech. Sci., vol. 71, no. 4, p. e145939, 2023

3

Fig. 3. Front view of DBP

Due to the usage of DBP, the flow path is rotational in the test section, and the flow in the test section turns into an ideal swirl pattern while passing over tube bundles. Due to the effect of α, the axial fluid flow is enhanced and transformed into a plug flow. Fluid flow with the deflector baffle is continuous, and no dead zones formations can be noted near the deflector baffle. The swirl motion improves mixing, and heat transfer in this region significantly improves at the expense of pressure drop.

The rotating air structures then introduce turbulence in the channel and generate vortices flowing past the tubes. However, the turbulence and flow rotation are governed by the distance between the baffle plates. Hence, the baffle plates' pitch ratio (P_R) has been tested for 0.8, 1, 1.2 and 1.4. To fix the deflectors onto the baffle plate, four trapezoidal openings with the bases (parallel sides) being 2d and 3d, respectively, and the legs (lateral sides) of lengths 8d have been provided, over which the trapezoidal deflectors of the exact dimensions have been fixed with the larger edge on the baffle plates that were inclined at an angle of (α) with the baffle plane in a circular array shown in Fig. 4. Three inclination angles, namely 30°, 40°, and 50°, are considered for the study.
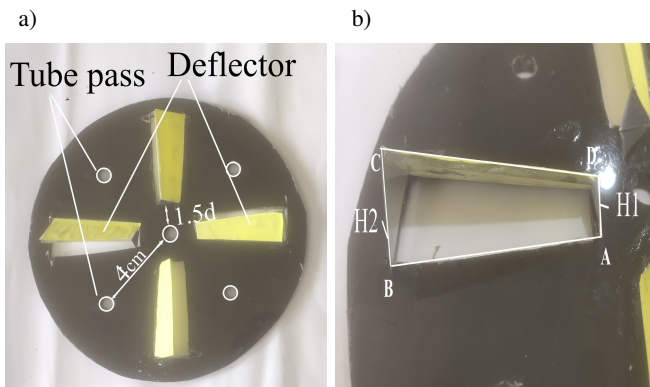
Fig. 4. a) DBP with five tube configurations, b) side view of DBP

The inclination of the deflectors to the baffle plate thus creates an opening for air passage, considered a flow area. These deflectors have been placed at a radial spacing of 1.5d from the center of the baffle plate, with d being copper tube ID = 8 mm. The deflector structure leads to a variation of height H1 and H2, as seen in Fig. 4b. The ratio of height (H1/H2) doesn't vary for α, and its value is 0.5.

2.3. Design parameter of investigation

The pitch ratio [16, 17] is calculated as:

$$P_R = \frac{l}{D}.$$

The blockage ratio [24] is calculated as:

$$B_R = \frac{S}{C}.$$

S – cross-sectional area of duct-($4\times$ cross-sectional area of the trapezoidal deflector), C – cross-sectional area of the duct, α – inclination angle (angle made by the deflector with baffle plane), H – deflector height ratio = $H1/H2$.

In the current study, three different sets of models for DBP are prepared and tested in a circular duct with a blockage ratio of ($B_R = 0.70$).

The different models and their geometric details are shown in Table 3.

Table 3
a) Model details

Model name ↓	D_h Hydraulic diameter in cm ↓	Inclination angle (degree) ↓	B_R Blockage ratio ↓
DBP1	1.87250	30	
DBP2	2.2475	40	0.70
DBP3	2.50239	50	

b) Sample details

Sample number →	1	2	3	4
Pitch ratio (P_R) →	0.8	1	1.2	1.4
Model name ↓				
DBP1	dbp11	dbp12	dbp13	dbp14
DBP2	dbp21	dbp22	dbp23	dbp24
DBP3	dbp31	dbp32	dbp33	dbp34

The result obtained from different samples is then compared to a smooth duct without DBP.

2.4. Data reduction

Cao's [25] method is used to evaluate the average convective heat transfer coefficient ($h_{c,m}$ in W/m²·K). The associated parameters are as follows:

The prominent equations for evaluating these parameters are as follows: Reynolds number (Re_d)

$$Re_d = \rho \cdot v \cdot D_h / \mu, \tag{1}$$

where v denotes average velocity in m/s, and D_h denotes the hydraulic diameter of the air duct in m.

$D_h = 4\times$ ($4\times$ Flow area) / Wetted perimeters.

4

Bull. Pol. Acad. Sci. Tech. Sci., vol. 71, no. 4, p. e145939, 2023

Investigations of the turbulent thermo-fluid performance in a circular heat exchanger with a novel flow deflector-type baffle plate

Wetted perimeter $= 5\times$ perimeter of the tube pass $+4\times$ perimeter of the deflector.

The thermal properties of air, such as ρ (density in kg/m^3) and μ (coefficient of dynamic viscosity in kg/m·s), are assessed using the average air-side intake and outlet bulk temperature values.

$$v = \sqrt{2\Delta P_o/\rho}\,, \tag{2}$$

$$h_{c,m} = Q/A_p \Delta t_{lm}\,, \tag{3}$$

where the heat transfer rate for the air-side is denoted by Q (in Watts), the heat transfer area of the copper tube is A_p (in m^2), ΔP_o (pressure drop at orifice plate in Pa), and Δt_{lm} is the LMTD between the air and wall of the copper tube.

Q is calculated as:

$$Q = C_p \rho v A_c \left(T_{a,\text{out}} - T_{a,\text{in}}\right), \tag{4}$$

where v is the average velocity of airflow; A_c is the area of the cross-section of the duct; $T_{a,\text{in}}$ and $T_{a,\text{out}}$ are the temperatures of the air entering and exiting the test section, respectively.

Δt_{lm} is given as:

$$\Delta t_{lm} = \left[\frac{(t_{w,\text{in}} - t_{a,\text{in}}) - (t_{w,\text{out}} - t_{a,\text{out}})}{\ln\left(t_{w,\text{in}} - t_{a,\text{in}}\right)/\left(t_{w,\text{out}} - t_{a,\text{out}}\right)} \right], \tag{5}$$

where $t_{w,\text{in}}$ and $t_{w,\text{out}}$ is the average temperature at the wall of the copper tube, with $t_{w,\text{in}}$ and $t_{w,\text{out}}$ at the inlet and outlet, respectively.

They are calculated as:

$$T_{w,\text{in}} = \left[\frac{\sum_1^5 T_{w,i} A_i}{A_p} \right]_{\text{in}},$$

$$T_{w,\text{out}} = \left[\frac{\sum_1^5 T_{w,i} A_i}{A_p} \right]_{\text{out}}. \tag{6}$$

The heat transfer element of the tested duct is indicated by subscript i, which is 1, 2, 3, 4 and 5, matching the locations of the thermocouples on the copper tube at the test section's inlet and outlet along the airflow direction. And A_i represents the heat transfer area of a heating element.

The average Nusselt number (Nu), friction factor (f), and Colburn factor (j) describe the duct flow and thermal characteristics.

$$\text{Nu} = \frac{h_{c,m} D_h}{\lambda}\,, \tag{7}$$

$$j = \frac{\text{Nu}}{\text{Re}_d \text{Pr}^{1/3}}\,, \tag{8}$$

$$f = \frac{2\Delta P D_h}{\rho v^2 L}\,, \tag{9}$$

where ΔP is the test section's pressure drop.

From equations (3) and (4):

$$h_{c,m} = \frac{C_p \rho v A_c (T_{a,\text{out}} - T_{a,\text{in}})}{A_p \Delta t_{lm}}\,. \tag{10}$$

Dimensionless factors like heat transfer enhancement (j/j_0), flow resistance (f/f_0) and thermo-fluid performance [$R = (j/j_0)/(f/f_0)$], respectively, were used. Where f_0 and j_0 are the measured friction factor, and the Colburn factor of a smooth duct is used as a benchmark, with j and f as the corresponding values of DBP installed air duct [26–29].

3. RESULTS AND DISCUSSION

3.1. Validation of experimental result

For experimental precision, the Nu and f obtained using the experiment are contrasted with correlation (equation (7) and (9)). Dittus–Boelter and Gnielinski correlation approximates the fluids' surface coefficient of heat transfer in clean, circular pipes with turbulent flow.

Nusselt number correlations:

a) Dittus and Boelter correlation [30]

$$\text{Nu} = 0.023\,\text{Re}_d^{4/5}\,\text{Pr}^{0.4} \quad \text{for } \text{Re}_d \geq 1 \times 10^4. \tag{11}$$

b) Gnielinski

$$\text{Nu} = \frac{(\xi/8)\,(\text{Re}_d - 1000)\,\text{Pr}}{\left[1 + 12.7(\xi/8)^{1/2}\left(\text{Pr}^{2/3} - 1\right)\right]}$$
$$\cdot \left[1 + \left(\frac{D_h}{L}\right)^{2/3}\right]\left(\frac{P_{rm}}{P_{rw}}\right)^{0.11}. \tag{12}$$

The correlation is valid for $0.5 \leq \text{Pr} \leq 2000$ and $4000 \leq \text{Re}_d \leq 10^6$, where ξ is calculated using the Filonienko relationship:

$$\xi = (1.82\log\text{Re}_d - 1.64)^{-2}.$$

Symbols P_{rm} and P_{rw} designate the Prandtl number at the bulk and wall temperature, respectively.

Friction factor correlation:

a) Blasius correlation

$$f = 0.316\,\text{Re}_d^{-0.25} \quad \text{for } \text{Re}_d \leq 10^5. \tag{13}$$

b) Colebrook–White correlation [31]

$$\frac{1}{\sqrt{f}} = 1.8\log\left(\frac{\text{Re}_d}{6.9}\right) \quad \text{for } \text{Re}_d\ 4000 \leq \text{Re} \leq 10^8. \tag{14}$$

Figure 5 shows agreement between experimental results and those obtained using correlation, ensuring the correctness of experimental outcome with an absolute deviation shown below in Table 4.
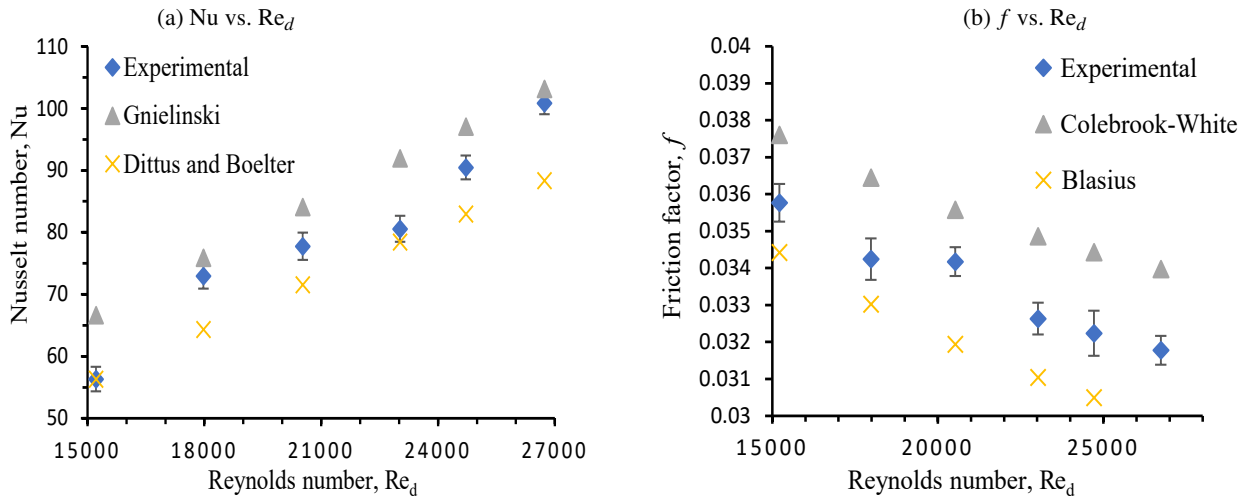
Bull. Pol. Acad. Sci. Tech. Sci., vol. 71, no. 4, p. e145939, 2023

5

(a) Nu vs. Re$_d$

(b) f vs. Re$_d$

Fig. 5. Comparison of average Nu and f for the smooth duct

Table 4

Average deviation of experimental values from empirical correlation

Nusselt number		Friction factor	
Correlation used ↓	Avg. deviation from experimental (in %)	Correlation used ↓	Avg. deviation from experimental (in %)
Dittus and Boelter	−7.185	Colebrook–White	+6.047
Gnielinski	+9.054	Blasius	−5.003

3.2. Heat transfer enhancement

A deflector baffle augments the heat transfer rate significantly under the given Re$_d$ range, which is a consequence of strong reverse flow (turbulence) and a thin boundary layer.

Figure 6 shows the variation in Colburn factor with Re$_d$. The j/j_o is highest at lower Re$_d$ but reduces steadily as the Re$_d$ increases and reaches a minimum value at Re$_d \sim 22000$, then gradually increases to up to Re$_d \sim 26500$ and then drops again. This trend in j/j_o is similar for all the samples of DBP. The DBP1 samples ($\alpha = 30°$) show the highest j/j_o values as compared to other inclination angles. This means that a significant fluctuation and disruption of the flow occurs at a smaller inclination angle. The disturbance intensity rises with a reduction
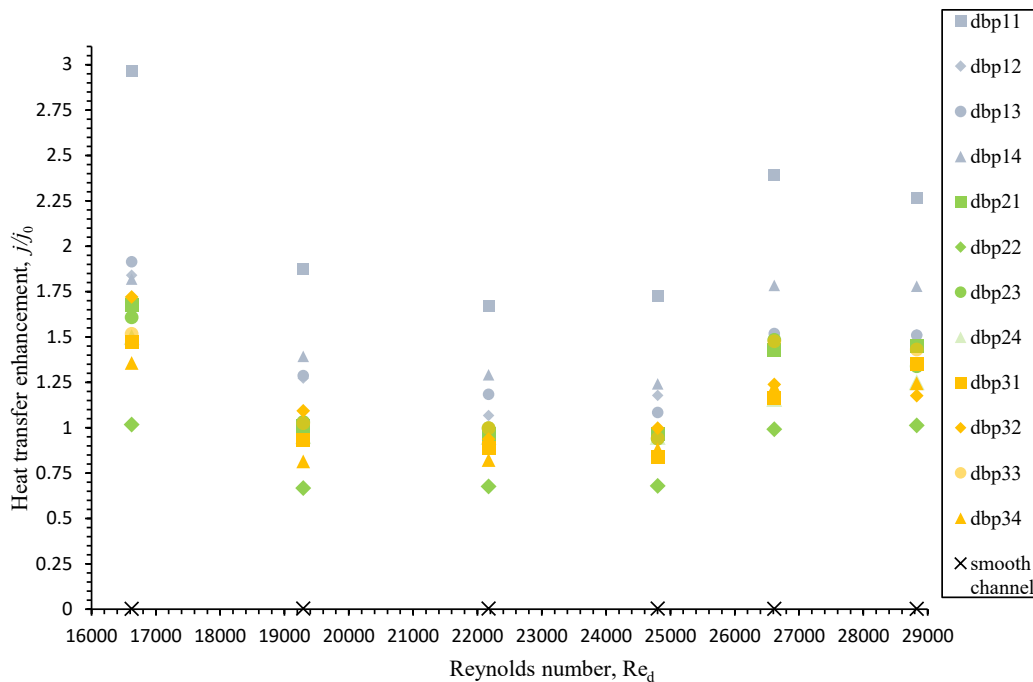

Fig. 6. Effect on heat transfer enhancement factor, j/j_o with the change in Reynolds number

6

Bull. Pol. Acad. Sci. Tech. Sci., vol. 71, no. 4, p. e145939, 2023

www.czasopisma.pan.pl PAN www.journals.pan.pl
POLSKA AKADEMIA NAUK

Investigations of the turbulent thermo-fluid performance in a circular heat exchanger with a novel flow deflector-type baffle plate

in α sub sequentially, producing stronger instability in the flow. Moreover, such a flow might hinder the thermal boundary layer, making it thinner and lowering the heat transfer resistance. The geometry of the deflector, which is inclined to the baffle plate, acts as a nozzle that accelerates fluid. The increase in velocity results in a rapid rise in interacting surface area for (air), leading to dissipation of dynamic air pressure at high viscosity loss near the tube and duct wall. Thus enhancing heat transfer performance at the expense of higher-pressure loss is unavoidable.

Wang et al.'s [32] investigation showed that for down-wash spacing vortex flow increases as flowing downstream. If the spacing is too small, vortex flows interaction is stronger, leading to frequent breakups of vortices, which is harmful to heat transfer enhancement. If this spacing is large, the vortex flow separates quickly without affecting the boundary layer formed on the down-wash. Also, higher pressure loss could result from the interaction of two closely spaced vortex flows. Thus, appropriate DBP spacing (P_R) is necessary to maximize heat transfer.

Figure 7 shows the average (j/j_0) fluctuation with P_R. The elevated turbulence intensity that the flow between the baffle plates experiences results in fluctuation in the heat transfer rate with varying P_R. It is observed that for a lower α value, the highest average (j/j_0) value is at a lower P_R value and it increases with an increase in the α value. A maximum of 2.14 for the Colburn factor is noted when $P_R = 0.8$ and $\alpha = 30$, shown in Fig. 7(a).
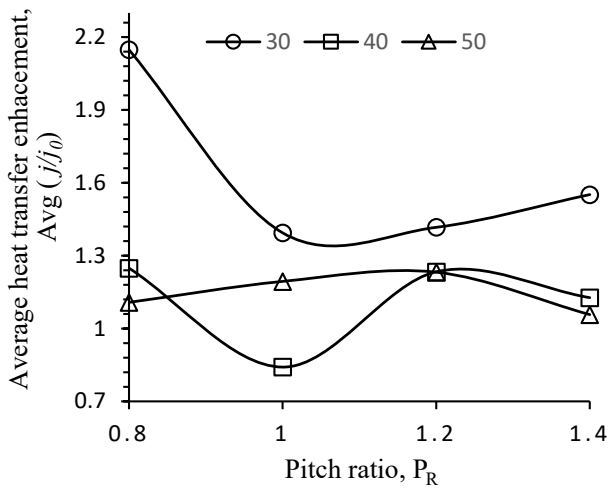
3.3. Flow resistance and thermo-fluid performance

The friction factor was obtained using equation (9). The relative friction factor (f/f_0) is plotted against the Re, as shown in Fig. 8. For a given range of Re_d, the duct equipped with DBP has a higher friction factor than the circular duct. It is observed that all DBP samples showed a similar trend, with its value being low at a low Reynolds number, then increasing gradually, attaining a peak value, then dropping. The highest relative friction factor is observed between the Re_d range of 24000–26000 as compared to other samples of DBP. As discussed above, a more significant airflow blockage and strong turbulence for the inclination angle (30°) enhances heat transfer, with a parallel negative impact on the frictional losses showcased by dbp11.
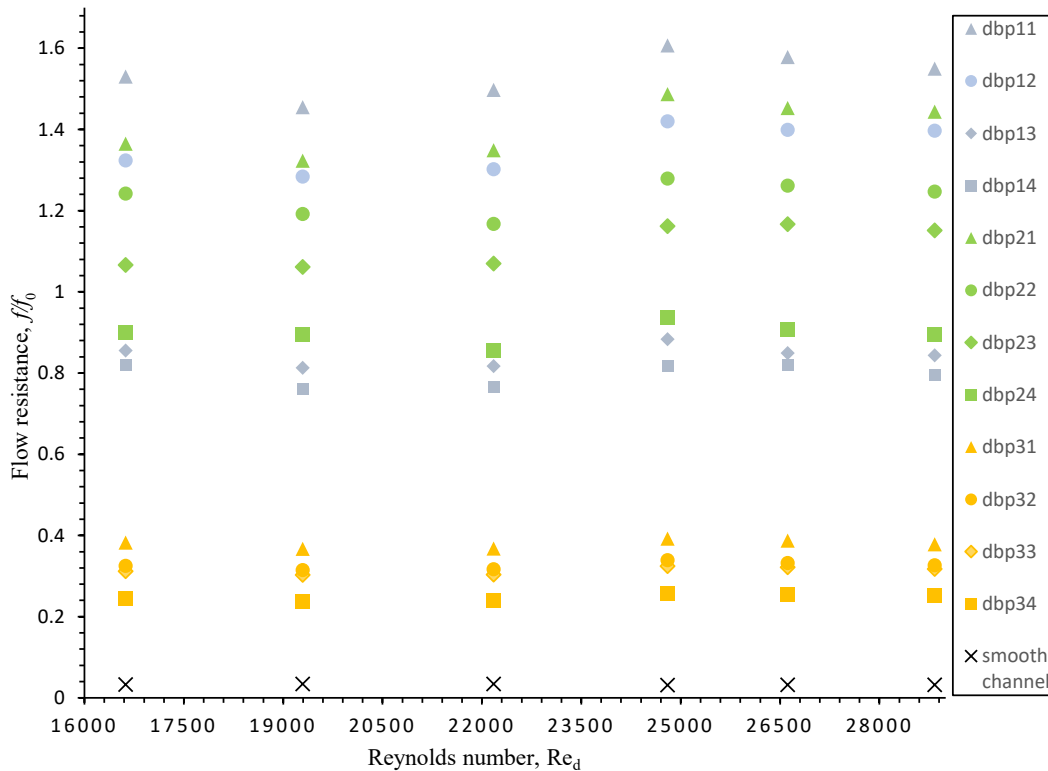

Fig. 7. Effect of Averaged (j/j_o) on PR

Fig. 8. Effect of f/f_0 on Re_d

Bull. Pol. Acad. Sci. Tech. Sci., vol. 71, no. 4, p. e145939, 2023

7

Pressure drops are always more pronounced in locations with higher velocities, stronger turbulence and longer fluid surface interaction. As a result, based on the prior study, it is anticipated that the pressure decrease will occur in the following order, from highest to lowest: DBP1, DBP2, DBP3, or (30°, 40°, 50°).

It is also seen in Fig. 9a that the average f/f_0 is higher for smaller P_R, smaller α, and achieving the maximum value of 1.536 for the $P_R = 0.8$ at $\alpha = 30$. The reason is possibly the fact that installation deflectors act as fluid obstructers, resulting in the pressure drop due to the loss in flow kinetic energy. The deflector with a minimum α value provides a powerful swirling flow, increasing the tangential contact between the secondary flow and the duct wall surface. The smaller P_R and smaller α cause more fluid turbulence and eventually more resistance to the flow, thus generating a more significant pressure drop and greater frictional forces. The combination $P_R = 0.8$ generates the highest f/f_0 at $\alpha = 30$, which is evident due to enormous turbulence/swirl flow by smaller α and more vigorous mixing by the number of baffle plates along the flow.

It can be seen from Fig. 9b that smaller inclination angles of DBP, such as $\alpha = 30°$, and $40°$, for thermo-fluid performance R, are lower as compared to larger inclination angles. For the given Re_d range, $\alpha = 50°$ presents the best thermo-fluid performance with R as high as 4.26 at $P_R = 1.4$. This is because with increas-

ing the inclination angle, the area facing the airflow increases, and then the pressure drop is rapidly reduced, along with a decline in velocity, particularly for intermediate Reynolds numbers (20000–24000), which strengthens the thermo-fluid performance of DBP.

4. CONCLUSIONS

An experimental analysis was carried out on a DBP fitted in a circular test section to study thermo-fluid characteristics such as j/j_o, f/f_0. and $(j/j_0)(f/f_0)$ for a turbulent regime. DBP augments the heat transfer capacity of air as it flows through the duct, but on the expanse of pressure drop, the heat transfer enhancement is a vital function of P_R and α.

Upon comparing different samples of DBP, it is noted that:

- Reduction in inclination angle leads to an average increase in flow velocity, with a 70.8% increase for 30°, 66.3% for 40°, and 61.3% increase for 50° as compared to a smooth duct.
- The average pressure drop is maximum for an inclination angle of 30° and reduces with an increase in the inclination angle by 75.50% for 30° and 61.17% for 40° and 48.14% for 50° as compared to a smooth duct.
- Average Nusselt numbers also show a decreasing trend, with its value decreasing by 54.9% for 30°, 33.14% for 40° and 22.55% for 50° as compared to a smooth duct.
- The average thermo-fluid performance values are 1.51 for 30°, 0.98 for 40°, and 3.69 for 50°.

APPENDIX I
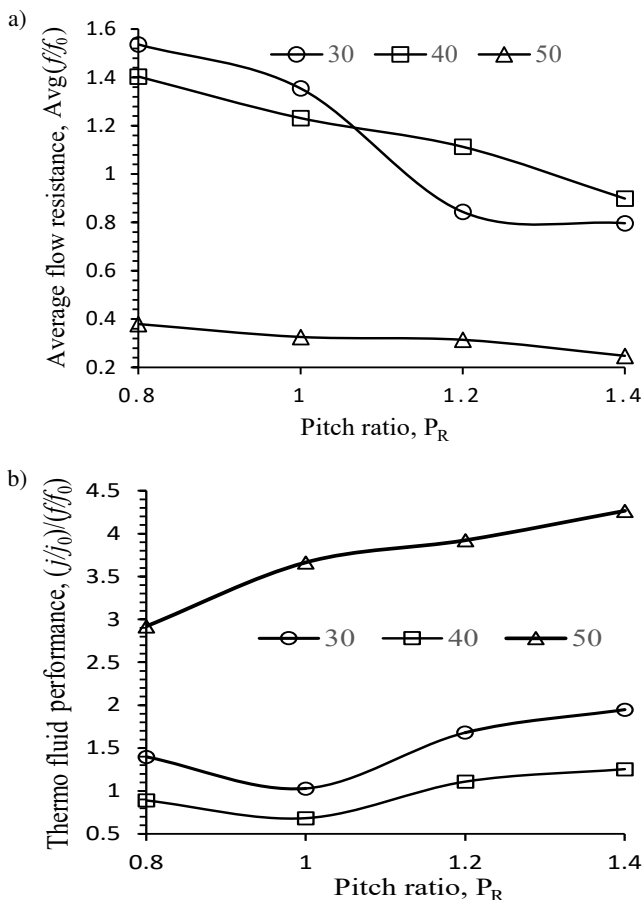
Table A1
Derived experimental values uncertainties

Parameters	Maximum uncertainties (%)
Reynolds number, Re_d	± 1.73
Nusselt number, Nu_m	± 2.35
Frontal velocity, v	± 6
Friction factor, f	± 4.22
Air-side heat transfer rate, Q	± 5

Fig. 9. Effect of α on (a) Average f/f_0 vs. P_R, (b) Reynolds average(j/j_0) (f/f_0) vs. P_R

REFERENCES

[1] R. Webb, *Principles of Enhanced Heat Transfer*. John Wiley & Sons, New York, 1994.

[2] A.E. Bergles, "Heat transfer enhancement – the encouragement and accommodation of high heat fluxes," *J. Heat Transf.-Trans. ASME*, vol. 119, no. 1, pp. 8–19, 1997, doi: 10.1115/1.2824105.

8

Bull. Pol. Acad. Sci. Tech. Sci., vol. 71, no. 4, p. e145939, 2023

Investigations of the turbulent thermo-fluid performance in a circular heat exchanger with a novel flow deflector-type baffle plate

[3] M. Sheikholeslami, M. Gorji-Bandpy, and D.D. Ganji, "Review of heat transfer enhancement methods: Focus on passive methods using swirl flow devices," *Renew. Sustain. Energy Rev.*, vol. 49, pp. 444–469, 2015, doi: 10.1016/j.rser.2015.04.113.

[4] A. Sohal, K. Kumar, and R. Kumar, "Heat transfer enhancement with channel surface roughness: A comprehensive review," *Proc. Inst. Mech. Eng., Part C-J. Mech. Eng. Sci*, vol. 236, no. 11, pp. 6308–6334, 2022, doi: 10.1177/095440622110656.

[5] K. Yakut and B. Sahin, "Flow-induced vibration analysis of conical rings used heat transfer enhancement in the heat exchanger," *Appl. Energy*, vol. 78, no. 3, pp. 273–88, 2004, doi: 10.1016/j.apenergy.2003.09.001.

[6] V. Kongkaitpaiboon, K. Nanan, and S. Eiamsa-ard, "Experimental investigation of convective heat transfer and pressure loss in a round tube fitted with circular-ring turbulators," *Int. Commun. Heat Mass Transf.*, vol. 37, pp. 568–574, 2010, doi: 10.1016/j.icheatmasstransfer.2009.12.016.

[7] F. Kreith and D. Margolis, "Heat transfer and friction in turbulent vortex flow," *Appl. Sci. Res.*, vol. 8, pp. 457–473, 1959.

[8] M. Tusar, K. Ahmed, and M. Bhuiya, "CFD study of heat transfer enhancement and fluid flow characteristics of laminar flow through tube with helical screw tape insert," *Energy Procedia*, vol. 160, pp. 699–706, 2019, doi: 10.1016/j.egypro.2019.02.190.

[9] Z.Y. Yang, "Enhanced condensation using twisted-tape inserts," in *6th ASME–JSME, Thermal Engineering Joint Conference*, USA, 2003.

[10] S. Eiamsa-ard and P. Promvonge, "Enhancement of heat transfer in a tube with regularly-spaced helical tape swirl generators," *Solar Energy*, vol. 78, no. 4, pp. 483–494, 2005, doi: 10.1016/j.solener.2004.09.021.

[11] R. Sethumadhavan and M.R. Rao, "Turbulent flow heat transfer and fluid friction in helical-wire-coil-inserted tubes," *Int. J. Heat Mass Transf.*, vol. 26, no. 12, pp. 1833–1845, 1983, doi: 10.1016/S0017-9310(83)80154-9.

[12] S.R. Chaurasia and R.M. Sarviya, "Comparative thermal hydraulic performance analysis on helical screw insert in tube with different number of trips in transition flow regime," *Heat Mass Transf.*, vol. 57, pp. 77–91, 2021.

[13] V.K. Dhir, F. Chang, "Heat transfer enhancement using tangential injection," *ASHRAE Trans.*, 1992, vol. 98, p. BA-92-4-1.1992.

[14] A. Durmus, A. Durmus, and M. Esen, "Investigation of heat transfer and pressure drop in a concentric heat exchanger with snail entrance," *Appl. Therm. Eng.*, vol. 22, no. 3, pp. 321–32, 2002, doi: 10.1016/S1359-4311(01)00078-3.

[15] M. Yilmaz, O. Comakli, and S. Yapici, "Enhancement of heat transfer by turbulent decaying swirl flow," *Energy Conv. Manag.*, vol. 40, pp. 1365–76, 1999, doi: 10.1016/S0196-8904(99)00030-8.

[16] M. Sheikholeslami, M.G. Bandpy, and D.D. Ganji, "Effect of discontinuous helical turbulators on heat transfer characteristics of double pipe water to air heat exchanger," *Energy Conv. Manag.*, vol. 118, pp. 75–87, 2016, doi: 10.1016/j.enconman.2016.03.080.

[17] M. Sheikholeslami and D.D. Ganji, "Heat transfer enhancement in an air-to-water heat exchanger with discontinuous helical turbulators; experimental and numerical studies," *Energy*, vol. 116, no. 1, pp. 341–352, 2016, doi: 10.1016/j.energy.2016.09.120.

[18] A.K. Gupta, D.G. Lilley, and N. Syred, *Swirl Flows*. Kent, England: Abaccus Press, 1984.

[19] P. Promvonge and S. Eiamsa-ard, "Heat transfer enhancement in a tube with combined conical-nozzle inserts and swirl generator," *Energy Conv. Manag.*, vol. 47, no. 18–19, pp. 2867–2882, 2006, doi: 10.1016/j.enconman.2006.03.034.

[20] T. Akiyama and M. Ikeda, "Fundamental study of the fluid mechanics of swirling pipe flow with air suction," *Ind. Eng. Chem. Process Des. Dev.*, vol. 25, no. 4, pp. 907–913, 1986, doi: 10.1021/i200035a012.

[21] M.L. Mathur and N.R.L. Macallum, "Swirling air jets issuing from vane swirlers, part 1: Free jets," *J. Inst. Fuel*, vol. 40, pp. 214–225, 1967.

[22] *ASHRAE Handbook – Fundamentals*, American Society of Heating, Refrigerating and Air-conditioning Engineers, SI-ed, Atlanta, ch. 13, 1993, pp. 14–15.

[23] H.W. Coleman and W.G. Steele, *Experimentation, validation, and uncertainty analysis for engineers*. John Wiley & Sons, 2018.

[24] J.D. Holmes, *Wind Loading of Structures*, 2nd ed., Taylor & Francis: New York, USA, 2007, pp. 168–169.

[25] Y.Z. Cao, *Experimental Heat Transfer*. 1st ed., National Defence Industry Press: Beijing, 1998, pp. 120–125.

[26] J. Ma, Y.P. Huang, J. Huang, Y.L. Wang, and Q.W. Wang, "Experimental investigations on single-phase heat transfer enhancement with longitudinal vortices in narrow rectangular channel," *Nucl. Eng. Des.*, vol. 240, no. 1, pp. 92–102, 2010, doi: 10.1016/j.nucengdes.2009.10.015.

[27] S. Eiamsa-ard, "Study on thermal and fluid flow characteristics in turbulent channel flows with multiple twisted tape vortex generators," *Int. Commun. Heat Mass Transf.*, vol. 37, no. 6, pp. 644–651, 2010, doi: 10.1016/j.icheatmasstransfer.2010.02.004.

[28] S.V. Garimella and P.A. Eibeck, "Enhancement of single-phase convective heat transfer from protruding elements using vortex generators," *Int. J. Heat Mass Transf.*, vol. 34, no. 9, pp. 2431–2433, 1991, doi: 10.1016/0017-9310(91)90068-P.

[29] M. Fiebig, "Review embedded vortices in internal flow: heat transfer and pressure loss enhancement," *Int. J. Heat Fluid Flow*, vol. 16, no. 5, pp. 376–388, 1995, doi: 10.1016/0142-727X(95)00043-P.

[30] F.W. Dittus and L.M.K. Boelter, "Heat Transfer in Automobile Radiators of the Tubular Type," University of California Press, Berkeley: University of California Publications in Engineering, vol. 2, pp. 443–461, 1930.

[31] F.M. White, *Fluid mechanics*. McGraw-Hill: Boston, 2003.

[32] J.L. Wang, Z.S. Zhang, and X. Zeng, "Effect of longitudinal vortices on the turbulent structure in near-wall region," *Acta Mech. Sin.*, vol. 26, no. 5, pp. 625–629, 1994.